ACS OMEGA

http://pubs.acs.org/journal/acsodf

Article

Optimization and Synthesis of a La-TMA MOF with Some Improvements in Its Properties

Zohreh Fateminia* and Hossein Chiniforoshan

Cite This: *ACS Omega* 2023, 8, 262−270

Read Online

ACCESS | Metrics & More | Article Recommendations | Supporting Information

ABSTRACT: A La-TMA metal−organic framework (MOF) made up of benzene-1,3,5-tricarboxylate and La(III) was synthesized by a different methodology compared to those in previous reports. By using various approaches, the structural characteristics and physical properties of the La-TMA MOF were analyzed. Eventually, the results showed micro-hexagonal hollow tubes with a high crystallinity grade and thermal stability (up to 400 °C) and a higher surface area compared with those from earlier reports. The BET surface area of a similar previous MOF was about 14.8 m^2/g; however, in the current project, the BET surface area increased to about 34.49 m^2/g and the Langmuir surface area to 42.3 m^2/g.

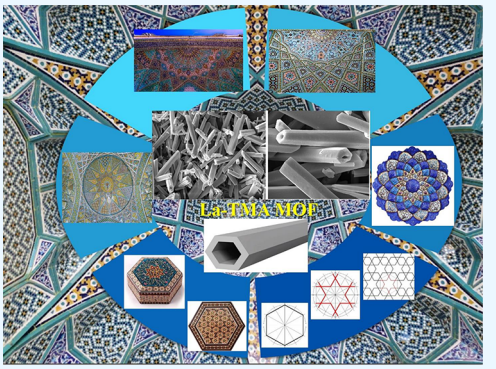

1. INTRODUCTION

Metal−organic frameworks (MOFs) are the types of penetrable crystalline hybrid materials, and these networks have achieved extraordinary growth over the last years, with growing importance in industry, more specifically in science and engineering. These compounds have been known as a pervasive branch of porous materials with crystalline architecture and enormous surface areas. MOFs comprise inorganic moieties or metal-based node centers (ions like alkaline earth metals, transition metals, lanthanides, or clusters) and organic moieties involving the extended family of some multifunctional ligands, which bind to each other through coordination bonds to make crystalline frameworks. The organic linkers are usually based on polytopic N-donor groups, carboxylates, or even phosphonates. However, different building blocks can be assembled to set up analogous structures, and as a way to solve the challenge of the random architecture and resultant behavior, post-synthetic modification of the synthesized product to provide a prospective network has been employed. It is an important area and promising strategy used to design and generate novel scaffolds for exhibiting stupendous properties compared to those of the parent frameworks. The changed chemical and physical properties induced in MOFs by changing their chemical composition have introduced unexampled opportunities for several applications.[1−3]

These arranged materials possess physicochemical parameters that result in desirable features, such as open metal sites, extraordinary surface area, large inoperative space, arranged topology structure, HOMO−LUMO level, pore size/shape, functionalized surface characteristics, uniform micro/nanopores,[4−6] and, finally, excellent thermal, mechanical, and chemical stability. The ability to control their morphology (like micro- or nanoscale spheres, cubes, sheets, and rods) and the chemical nature of their pores and to diversify the building blocks of these structures enables us to synthesize extraordinary MOFs with great potential for applications in energy such as storage media for gases and high-capacity adsorption/separation or in catalysis, dye/toxic material removal,[7−16] enzyme immobilization,[17] sensing, biomedicine and drug delivery,[18,19] separation, luminescence, fuel/energy conversion/storage, thin-film devices, membranes, ferroelectrics, and so on.[1,2,5,20−28]

Various methods have been suggested for synthesis of MOFs to achieve essential properties such as shape and morphology. The main purpose is to present an alternative method for preparing MOFs, utilizing a proper technique and optimizing the morphology or other properties through various factors, such as the concentration of reagents, reaction time, and different solvents. To date, various methods of MOF preparation in the laboratory and industry have been reported, from conventional solvothermal/hydrothermal synthesis to microfluidic synthesis or dry gel conversion, etc.[20,29−32] These materials have had great effects on a broad range of groundbreaking research areas and also industries. Moreover,

Received: June 25, 2022
Accepted: October 20, 2022
Published: December 29, 2022

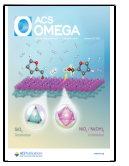

https://doi.org/10.1021/acsomega.2c03973
ACS Omega 2023, 8, 262−270

Table 1. Comparison of La-Based MOFs Comprising 1,3,5-Tricarboxylic Acid Linkers

	conditions				
name of MOF	solvent/solvents	temperature	reaction time	unit cell	morphology
La-TMA MOF[a]	DMF/formic acid (1:1)	100 °C	12 h	monoclinic	hexagonal hollow tube
$La(BTC)(H_2O)_6$[38]	DMF/water (1:1)	room temperature	6 h	monoclinic	spindly rectangular rods
$La(1,3,5\text{-}BTC)(H_2O)_6$[34]	HNO_3, water, ethanol	room temperature	15 min	monoclinic	3D flowerlike
La-BTC[39]	DMF	120 °C	24 h		rod-like
$La(BTC)(DMF)_2(H_2O)$ or LaMOF[40]	DMF/water	65 °C	24 h	monoclinic	rod-like
$La(BTC)(H_2O)(DMF)$[41]	DMF	150 °C	36 h	monoclinic	rod-like

[a]This project.

conditional and environmental challenges such as high temperature, the presence of toxic organic solvents and their types, and excessively acidic or basic pH are the most important parameters.[33] The most common solvothermal synthesis necessitates non-renewable solvents, organic compounds, and high boiling temperatures. However, MOFs are mostly synthesized by solvothermal design, which involves poisonous solvents, long procedure times, and environmental and health complications, although the effort to develop green synthesis techniques is a welcome occurrence. Different parameters of MOF synthesis such as reagents, concentrations, molar ratios, surfactants, and solvents can lead to different 3D structures of MOFs.[34] One of the most important steps in the synthesis is the selection of a solvent (or solvents) that is a structure-directing agent and will regularize the coordination environment. As a result, the kind of solvent has a significant influence over the resulting lattice structure. Of course, the use of some organic solvents can damage the environment.[35,36]

Computational assessments have proved that the thermal stability of MOFs is the counterpart with 1- coordination number and 2- coordination environment (not with framework topology).[37] The specific heat capacities (C_p) of all MOFs that were studied by Mu and Walton are comparable with those of solid-state materials such as coordination polymers, zeolites, carbon nanotubes, and minerals. Among these MOFs, the one with the highest thermal stability is LaBTB (560 °C) as a result of the high coordination number of La, which is common among lanthanides.[37]

La-based MOFs with different conditions of synthesis have been reported many times. Of course, their obtained products have some differences. Some of these differences and their unit cells are shown in Table 1.[34,38−41] A La(BTC) with a micro-spindly rectangular rod shape and some of its graphene oxide composites were synthesized by Liu et al., which had BET surface areas of 14.8 m^2/g for the MOF and, as the best result, 26.6 m^2/g for its graphene oxide composite. Furthermore, they acted as good absorbents for proteins (especially for hemoglobin).[38] La-based MOFs have been used as purifier agents for water and air several times. Zhang et al. used the calcination process on a La(BTC) MOF to absorb phosphate from water, which could remove more than 170 mg P/g phosphate from water.[42] In addition, Jeyaseelan et al. prepared a composite of hydroxyapatite as a substrate with a La(BTC) MOF as a layer on it for defluoridation of water.[43] The two La^{3+}-based MOFs that had been prepared by Paz et al. were thermally stable MOFs (up to 400 °C) and had high selectivity for absorbing CO_2 and not N_2 gas.[44] Now, we introduce another micro-La-TMA MOF with a novel hexagonal hollow tube shape to this class of MOFs.

2. REAGENTS AND INSTRUMENTS

All of the chemical precursors and solvents were of analytical grade and supplied by commercial sources. They were used as received without further purifications. Benzene-1,3,5-tricarboxylic acid, $La(NO_3)_3{\cdot}6H_2O$, and solvents comprising dimethylformamide (DMF) and formic acid were purchased from the company Sigma-Aldrich. Fourier transfer infrared (FT-IR) spectra were obtained by a Rayleigh WQF-510A FT-IR spectrometer (400−4000 cm^{-1}) using KBr pellets. Field emission scanning electron microscopy (FE-SEM), energy-dispersive X-ray spectroscopy (EDS), and elemental mapping were carried out with a Quanta FEG 450 FEI. The results of thermogravimetry (TG) and differential scanning calorimetry (DSC) were recorded using a TA thermogravimeter, the Q600. Powder X-ray diffraction (XRD) analysis was carried out by means of an ASENWARE AW-XDM 300 with a step time of 1 s and a step size of 0.05° at 40 kV, 30 mA, and a 0.154184 nm wavelength. The surface area, adsorption/desorption graph, and corresponding data of the La-TMA MOF were obtained by a BELSORP-mini II. And as the other technique, X-ray photoelectron spectroscopy results were obtained using a Bes Tec in a 10^{-10} mbar vacuum with Kα energy = 1486.6 eV and an Al anode.

3. EXPERIMENTAL SECTION

Benzene-1,3,5-tricarboxylic acid (0.0417 g, 0.198 mmol) and $La(NO_3)_3{\cdot}6H_2O$ (0.086 g, 0.198 mmol) at a 1:1 molar ratio were mixed in an autoclavable glassy container that contained 10 mL of formic acid and 10 mL of pure DMF (at a 1:1 voluminal ratio). we shook the dish of the mixture for a few seconds to dissolve the reagents, and then it was put in an oven at 100 °C for 12 h. Then, the product was collected and sequentially washed with 5 mL of pure DMF, 5 mL of deionized water, and 5 mL of absolute acetone. Then, the white precipitate was put in an oven at 50 °C for 30 min to remove the residual solvents. The efficiency was more than 80%.

4. THE CHARACTERIZATION METHODS OF THE MATERIAL

4.1. FT-IR Spectroscopy. The selected infrared absorption bands (KBr, cm^{-1}) are listed in Table 2.[45] Great transformations in the FT-IR pattern of the La-TMA MOF versus that of the pure ligand were observed, which demonstrated the formation of a TMA-bonded-to-La structure.

4.2. Powder X-ray Diffraction. Normal powder XRD was utilized to find out the class of the crystalline structure with the parameters of the La-TMA MOF (Figure 1b). The unit cell of La-TMA MOF was determined to be monoclinic, with space

https://doi.org/10.1021/acsomega.2c03973
ACS Omega 2023, 8, 262−270

Table 2. The Main FT-IR Absorption Bands of the La-TMA MOF

functional group and vibrational mode	reference wavenumber of the moieties (cm^{-1})	La-TMA MOF (cm^{-1})
O−H stretching vibration	>3500 (m, very broad)	3442 (m, very broad)
C−H aromatic stretching vibration	3000−3100	2908, 3001 (w)
C═C and	1650−1690	1408, 1421
C═O stretching vibration	1660−1740 (vs)	1577 (vs)
aryl C−H out-of-plane bending (or wag) vibration	795−880	773 (s)

group $I12/c1$ and cell specifications a = 7.621(6) Å, b = 5.368(4) Å, c = 3.596(2) Å, $\alpha = \gamma = 90°$, and β = 96.73(1)°.

4.3. X-ray Photoelectron Spectroscopy. X-ray photoelectron spectroscopy (XPS) is a reliable method for comprehensive study of materials and is especially suited for surveying coordination compounds.[46,47] The full-survey spectrum of the La-TMA MOF coordination polymer is shown in Figure 2a, where each of the main peaks is deconvoluted to La 3d, La 4p, O 1s, and C 1s zones, confirming the existence of a trimesic acid ligand and metal components in the product. However, we will assess its XPS pattern in detail in the Results and Discussion section.

4.4. Morphological Properties of the La-TMA MOF; SEM, EDS, and Elemental Mapping. The surface features of the La-TMA MOF were scrutinized by the FE-SEM, EDS, and elemental mapping techniques. The SEM images are given in Figure 3a,b.

4.5. Thermogravimetry Analysis and DSC. To estimate the thermal stability of the La-TMA MOF, TG (thermogravimetry analysis (TGA) and its derivative, DTG) as well as DSC measurements were performed and their results are depicted in Figure 4a,b. TGA and DSC were carried out at a 15 °C/min heating rate. Both thermostability assessments were performed under a nitrogen atmosphere, in the temperature range ∼28−850 °C.

4.6. The Surface Area Studies. The surface area and behavior of the nitrogen gas adsorption/desorption of the La-TMA MOF was studied. The profiles of such behavior and surface area of the MOF were computed using Brunauer−Emmett−Teller (BET) calculations.

5. RESULTS AND DISCUSSION

The selected IR absorption bands (Table 2) exhibit great transformations in the FT-IR pattern of the La-TMA MOF versus the those of the pure ligand, which verified the formation of a TMA-bonded-to-La structure. The normal powder XRD showed the monoclinic unit cell of the La-TMA MOF, with an $I12/c1$ space group and a = 7.621(6) Å, b =

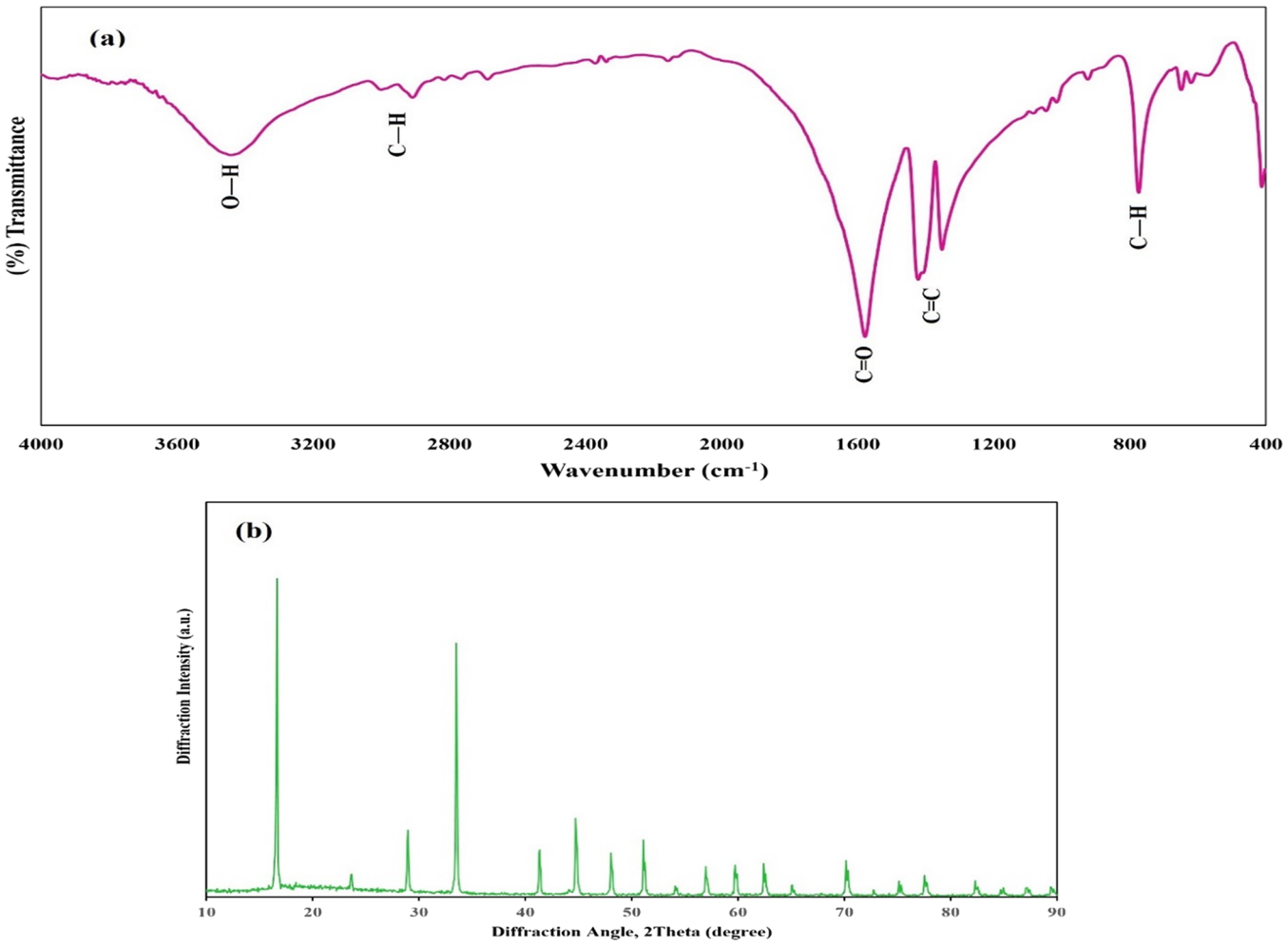

Figure 1. (a) FT-IR spectrum and (b) XRD pattern of the La-TMA MOF.

https://doi.org/10.1021/acsomega.2c03973
ACS Omega 2023, 8, 262−270

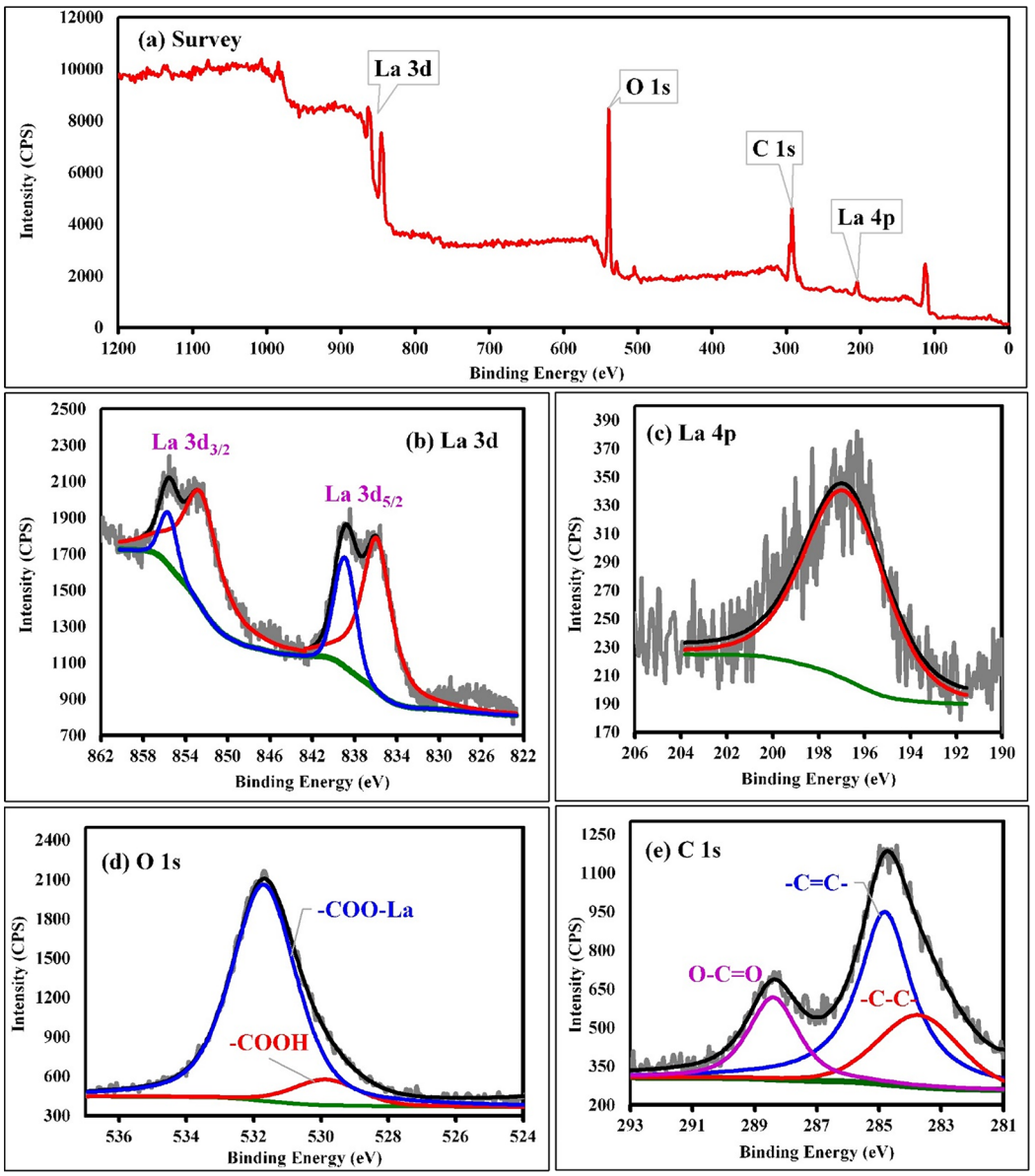

Figure 2. (a) XPS survey spectrum of La-TMA MOF and detailed spectra of (b) La 3d, (c) La 4p, (d) O 1s, and (e) C 1s (e) atoms in the La-TMA MOF.

5.368(4) Å, c = 3.596(2) Å, $\alpha = \gamma = 90°$, and β = 96.73(1)° cell parameters. The XPS of the La-TMA MOF showed the deconvoluted La 3d spectrum (Figure 2b). The XPS spectrum of La 3d has two main peaks of La $3d_{3/2}$ and La $3d_{5/2}$ at binding energies of 852.5 and 835.8 eV, respectively, and the difference between the two major peaks is 16.7 eV, as confirmed by the pattern in the spectrum of lanthanum.[48,49] Further, the other two peaks at 838.8 and 855.5 eV are La 3d satellite peaks, which are set down to the relocation of electrons of O 2p to an unoccupied La 5f revealing the La^{3+} oxidation state.[50] Figure 2c displays the high-resolution La 4p XPS spectrum of the La-TMA MOF compound, which has a peak observed at a binding energy of 196.8 eV.[51] The deconvolution of O 1s is displayed in Figure 2d. There are two types of oxygen present in the surface of the La-TMA MOF with BEs of 529.8 and 531.7 eV, which could be assigned to oxygen atoms in the patterns of −(C═O)OH and −COO−La, respectively.[52] The two oxygen atoms in the carboxylate (COO−) moiety bound to La(III) might be equivalent.[53] Figure 2e displays the high-resolution C 1s XPS spectrum of the La-TMA MOF, which is fitted into three peaks at 283.7, 284.6, and 288.3 eV. The peaks at 283.7 and 284.6 eV are assigned to the C═C and C−C bonds of trimesic acid ligands. Another peak (at 288.3 eV) would be ascribed to the −(C═O)OH bond of the ligand.[48] The results of SEM, EDS, and elemental mapping studies obviously indicated hollow hexagonal tubes with micrometer dimensions, lengths of several micrometers, and uniform shapes. The presence of C, O, and especially La atoms in the La-TMA MOF was analyzed by EDS (Figure 3a,b).[54,55] The peaks reveal the presence of La, O, and C atoms. The uniformity of elemental distributions was examined though elemental mapping analysis. In Figure 3c−f shown is the equally uniform distribution of all elements. A little bit of physically adsorbed molecules and solvents that were trapped in the pores of open channels in the main backbone of the La-TMA MOF, during the heating procedure and by increasing the temperature,[56−62] were removed the framework, simultaneously (this step is an endothermic

https://doi.org/10.1021/acsomega.2c03973
ACS Omega 2023, 8, 262−270

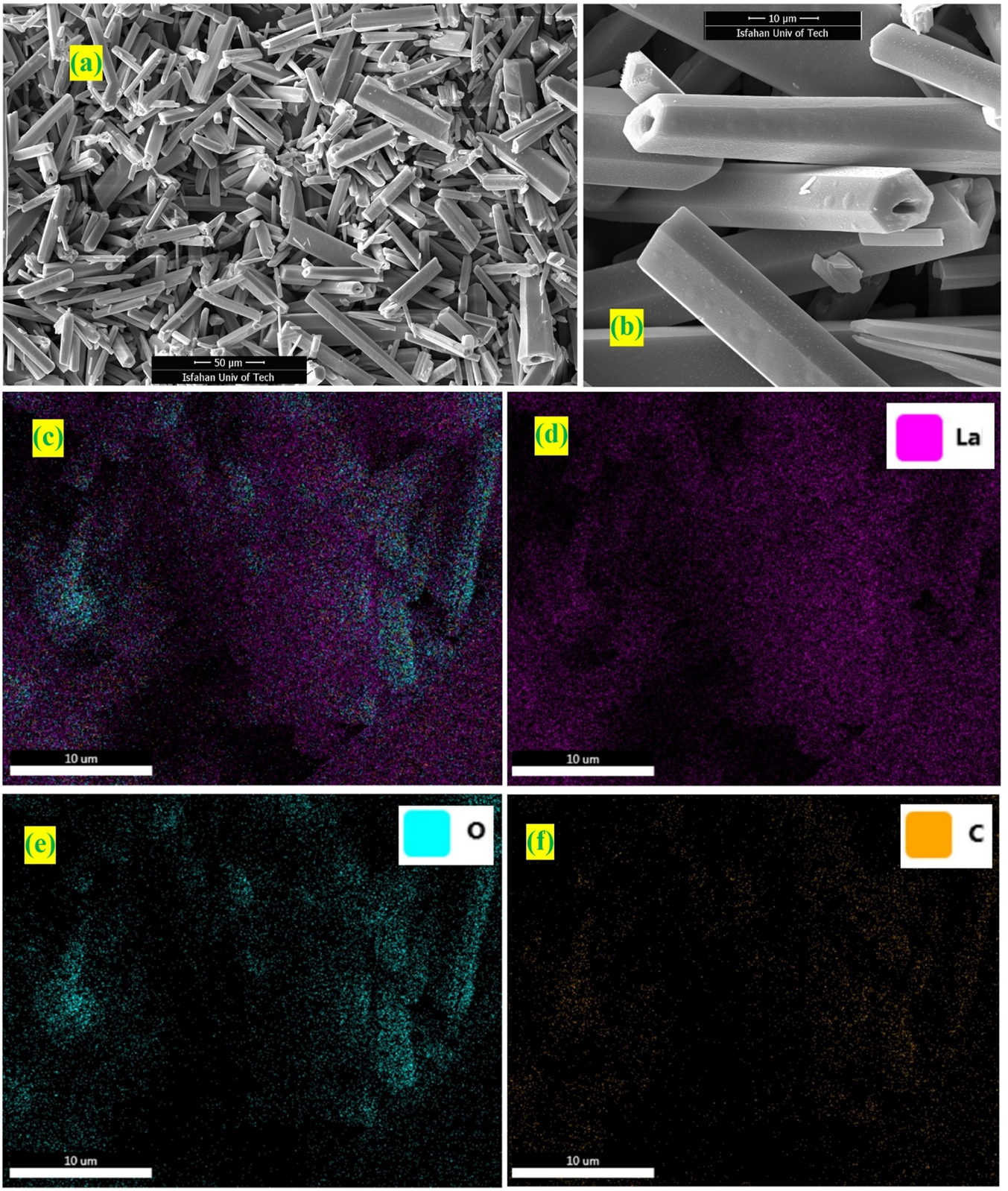

Figure 3. (a,b) SEM images of La-TMA MOF as well as (c–f) elemental mapping analysis of the La-TMA MOF.

procedure as exhibited in the DSC curve that is shown in Figure 4b). The onset decomposition temperature of the La-TMA MOF is ∼350 °C, and the peak is at 405.86 °C as shown in the TGA/DTG curves of the La-TMA MOF (Figure 4a). Hence, this MOF is thermally stable at least up to 350 °C. The uptake of nitrogen gas by the MOF was 7.9235 cm^3/g (STP), and also the pore volume was 0.3581 cm^3/g. The BET and Langmuir surface areas were 34.487 and 42.294 m^2/g, respectively (Table 3). The nitrogen adsorption/desorption behavior of the La-TMA MOF, which is shown in Figure 4c, represents a type IV isotherm and H1 hysteresis comprising narrow/uniform mesopores.[63]

https://doi.org/10.1021/acsomega.2c03973
ACS Omega 2023, 8, 262−270

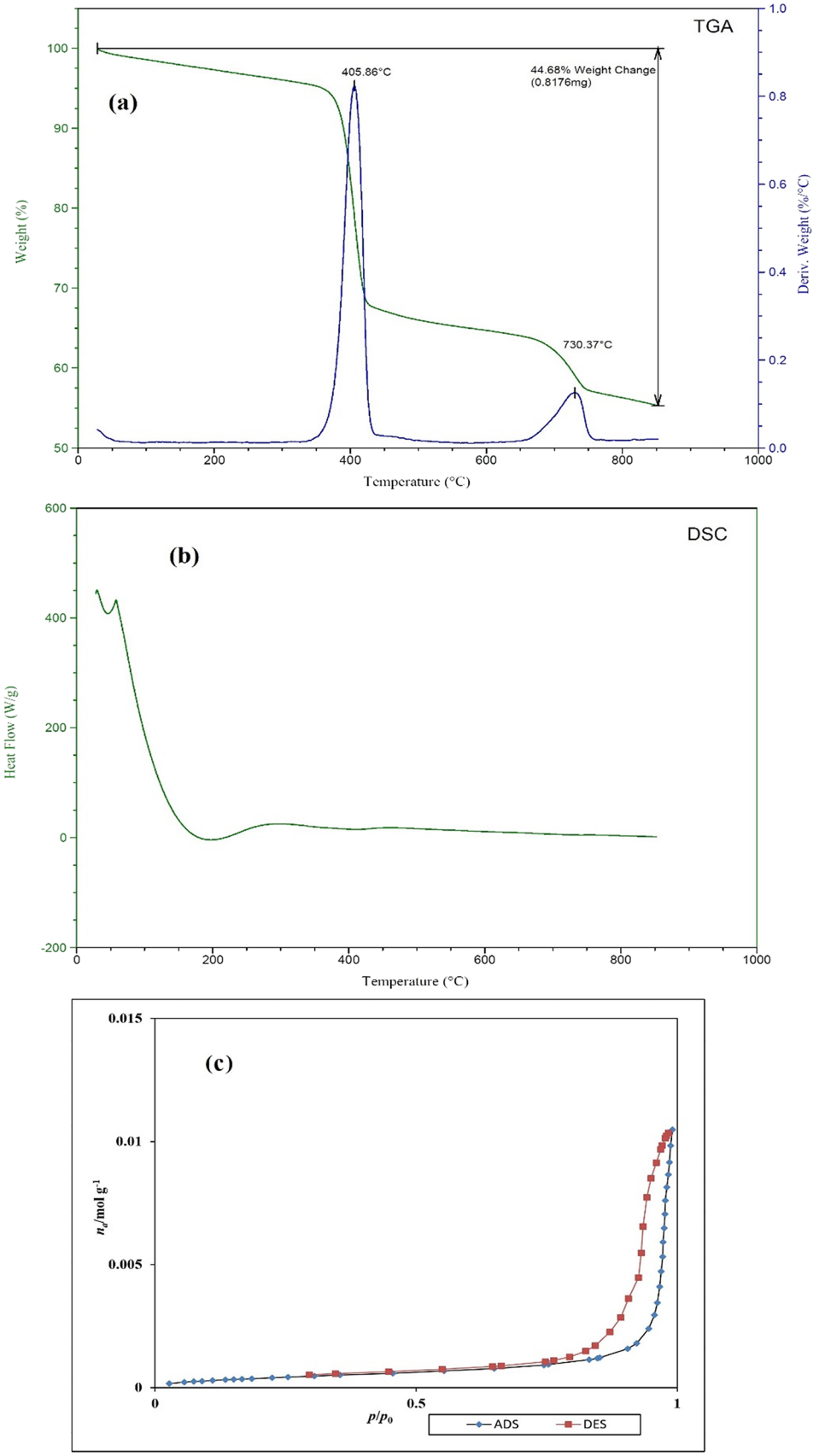

Figure 4. (a) Schemas of TG (green) and DTG (dark blue) of the La-TMA MOF and (b) DSC and (c) adsorption (blue)/desorption (orange) of the La-TMA MOF.

https://doi.org/10.1021/acsomega.2c03973
ACS Omega 2023, 8, 262−270

Table 3. The Resultant Data of La-TMA MOF BET and Langmuir Computations

BET plot		
V_m	7.9235	[cm^3(STP) g^{-1}]
$a_{s,BET}$	34.487	[m^2 g^{-1}]
mean pore diameter	41.532	[nm]
Langmuir plot		
V_m	9.7166	[cm^3(STP) g^{-1}]
$a_{s,Lang}$	42.291	[m^2 g^{-1}]

Consequently, this La-TMA MOF was synthesized by a comparatively facile method. Clearly, the characterization approaches delineate the formation of a pure, crystalline, and thermally stable La-based MOF with high efficiency. Liu et al. could prepare a $La(BTC)(H_2O)_6$ MOF and its graphene oxide composites with BET surface areas of 14.8 and 26.6 m^2/g as the best results, respectively.[38] However, the La-TMA MOF in this project has BET and Langmuir surface areas of 34.487 and 42.294 m^2/g, respectively.

The La-TMA MOF in this project is a thermally stable material (up to 400 °C) because of the high coordination number of La, which is common for lanthanide elements.[37] However, the TGA diagrams of La-TMA MOFs that were previously synthesized showed lower thermal stability[38,64] in comparison with that of our MOF.

Selection of solvent/solvents is a vital step in the solvothermal synthesis of MOFs and can regularize the coordination environment and have a structure-directing role. In this project, we chose DMF as well as formic acid, which have high boiling points and are common solvents in MOF preparation.[36] The obtained MOF has a micro-hexagonal hollow tube shape, which is a novel structure in the group of La-based MOFs. As previously described, this La-TMA MOF can be important in the absorption of proteins (especially hemoglobin (Hb)) with more than double the BET surface area in comparison to those of spindly rectangular rods from a previous work (14 m^2/g changes to 34 m^2/g)[38] or for phosphate absorption[42] and defluoridation of water[43] as well as absorption of CO_2.[44] Furthermore, the La-TMA MOF can be used as thermally stable material. As a result, La-based MOFs have the capacity to be studied more and more and used as a science-based industrial product.

6. CONCLUSIONS

In the current project, by using a new procedure, a La-TMA MOF with good purity and high efficiency in the class of La-based MOFs and desirable thermal stability (~ 400 °C) was synthesized. The construction of this MOF as well as some of its physical properties was verified through FT-IR, elemental analysis (CHN), FE-SEM, EDS, elemental mapping, XPS, XRD, DSC, TGA and DTG, and BET and nitrogen gas adsorption/desorption analyses. A MOF with a novel micro-hexagonal hollow tube shape in the class of La-based MOFs with high thermal stability, high quality of crystallinity, and a higher surface area in comparison to those from other research studies and with other considerable features was synthesized. Furthermore, the surface area from a previous work was ~14 m^2/g, which changes to ~34 m^2/g in the current project (increasing by about 20 m^2/g). Furthermore, this class of MOFs has an absorption capacity for CO_2 and contaminants from water.

ASSOCIATED CONTENT

Supporting Information

The Supporting Information is available free of charge at https://pubs.acs.org/doi/10.1021/acsomega.2c03973.

The XRD diagram and parameters well as elemental analysis (CHNS) of the La-TMA MOF are given in detail in the Supporting Information file (PDF)

AUTHOR INFORMATION

Corresponding Author

Zohreh Fateminia − *Department of Chemistry, Isfahan University of Technology, Isfahan, Iran 84156-83111;* orcid.org/0000-0002-7952-6245; Email: z.fateminia@ch.iut.ac.ir

Author

Hossein Chiniforoshan − *Department of Chemistry, Isfahan University of Technology, Isfahan, Iran 84156-83111*

Complete contact information is available at: https://pubs.acs.org/10.1021/acsomega.2c03973

Author Contributions

Z.F. was responsible for data curation, formal analysis, investigation, methodology, and writing. H.C. was responsible for funding acquisition, project administration, resources, supervision, and visualization.

Notes

The authors declare no competing financial interest.

ACKNOWLEDGMENTS

We greatly appreciate the financial support of the Isfahan University of Technology (IUT).

ABBREVIATIONS

TMA	trimesic acid or benzene-1,3,5-tricarboxylic acid
m	medium
w	weak
vs	very strong
s	strong
H_3BTB	1,3,5-tris-(4-carboxyphenyl)benzene

REFERENCES

(1) Zhou, H. C.; Long, J. R.; Yaghi, O. M. Introduction to metal−organic frameworks. *Chem. Rev.* **2012**, *112*, 673−674.

(2) Mandal, S.; Natarajan, S.; Mani, P.; Pankajakshan, A. Post-Synthetic Modification of Metal−Organic Frameworks Toward Applications. *Adv. Funct. Mater.* **2021**, *31*, 2006291.

(3) Du, M.; Li, Q.; Zhao, Y.; Liu, C. S.; Pang, H. A review of electrochemical energy storage behaviors based on pristine metal−organic frameworks and their composites. *Coord. Chem. Rev.* **2020**, *416*, No. 213341.

(4) Lai, H.; Li, G.; Xu, F.; Zhang, Z. Metal−organic frameworks: opportunities and challenges for surface-enhanced Raman scattering−a review. *J. Mater. Chem. C* **2020**, *8*, 2952−2963.

(5) Ismail, M.; Bustam, M. A.; Yeong, Y. F. Gallate-based metal−organic frameworks, a new family of hybrid materials and their applications: a review. *Crystals* **2020**, *10*, 1006.

(6) Furukawa, H.; Müller, U.; Yaghi, O. M. "Heterogeneity within order" in metal−organic frameworks. *Angew. Chem., Int. Ed.* **2015**, *54*, 3417−3430.

(7) Abdollahi, N.; Masoomi, M. Y.; Morsali, A.; Junk, P. C.; Wang, J. Sonochemical synthesis and structural characterization of a new Zn

(II) nanoplate metal−organic framework with removal efficiency of Sudan red and Congo red. *Ultrason. Sonochem.* **2018**, *45*, 50−56.
(8) Abbasi, A. R.; Yousefshahi, M.; Azadbakht, A.; Morsali, A.; Masoomi, M. Y. Methyl orange removal from wastewater using $[Zn_2(oba)_2(4\text{-bpdh})]\cdot$ 3DMF metal−organic frameworks nanostructures. *J. Inorg. Organomet. Polym. Mater.* **2015**, *25*, 1582−1589.
(9) Glover, T. G.; Peterson, G. W.; Schindler, B. J.; Britt, D.; Yaghi, O. MOF-74 building unit has a direct impact on toxic gas adsorption. *Chem. Eng. Sci.* **2011**, *66*, 163−170.
(10) Eltaweil, A. S.; Abd El-Monaem, E. M.; Omer, A. M.; Khalifa, R. E.; Abd El-Latif, M. M.; El-Subruiti, G. M. Efficient removal of toxic methylene blue (MB) dye from aqueous solution using a metal-organic framework (MOF) MIL-101 (Fe): isotherms, kinetics, and thermodynamic studies. *Desalin. Water Treat.* **2020**, *189*, 395−407.
(11) DeCoste, J. B.; Demasky, T. J.; Katz, M. J.; Farha, O. K.; Hupp, J. T. A UiO-66 analogue with uncoordinated carboxylic acids for the broad-spectrum removal of toxic chemicals. *New J. Chem.* **2015**, *39*, 2396−2399.
(12) Mondloch, J. E.; Katz, M. J.; Isley Iii, W. C.; Ghosh, P.; Liao, P.; Bury, W.; et al. Destruction of chemical warfare agents using metal−organic frameworks. *Nat. Mater.* **2015**, *14*, 512−516.
(13) Bobbitt, N. S.; Mendonca, M. L.; Howarth, A. J.; Islamoglu, T.; Hupp, J. T.; Farha, O. K.; Snurr, R. Q. Metal−organic frameworks for the removal of toxic industrial chemicals and chemical warfare agents. *Chem. Soc. Rev.* **2017**, *46*, 3357−3385.
(14) Martínez-Ahumada, E.; López-Olvera, A.; Jancik, V.; Sánchez-Bautista, J. E.; González-Zamora, E.; Martis, V.; Williams, D. R.; Ibarra, I. A. MOF Materials for the Capture of Highly Toxic H_2S and SO_2. *Organometallics* **2020**, *39*, 883−915.
(15) Islamoglu, T.; Chen, Z.; Wasson, M. C.; Buru, C. T.; Kirlikovali, K. O.; Afrin, U.; Mian, M. R.; Farha, O. K. Metal−organic frameworks against toxic chemicals. *Chem. Rev.* **2020**, *120*, 8130−8160.
(16) Bhattacharya, S.; Bala, S.; Mondal, R. Design of chiral Co (II)-MOFs and their application in environmental remediation and waste water treatment. *RSC Adv.* **2016**, *6*, 25149−25158.
(17) Liang, S.; Wu, X. L.; Xiong, J.; Zong, M. H.; Lou, W. Y. Metal-organic frameworks as novel matrices for efficient enzyme immobilization: an update review. *Coord. Chem. Rev.* **2020**, *406*, No. 213149.
(18) Shen, M.; Forghani, F.; Kong, X.; Liu, D.; Ye, X.; Chen, S.; Ding, T. Antibacterial applications of metal−organic frameworks and their composites. *Compr. Rev. Food Sci. Food Saf.* **2020**, *19*, 1397−1419.
(19) McKinlay, A. C.; Morris, R. E.; Horcajada, P.; Férey, G.; Gref, R.; Couvreur, P.; Serre, C. BioMOFs: metal−organic frameworks for biological and medical applications. *Angew. Chem., Int. Ed.* **2010**, *49*, 6260−6266.
(20) Vaitsis, C.; Sourkouni, G.; Argirusis, C. Metal organic frameworks (MOFs) and ultrasound: a review. *Ultrason. Sonochem.* **2019**, *52*, 106−119.
(21) Safaei, M.; Foroughi, M. M.; Ebrahimpoor, N.; Jahani, S.; Omidi, A.; Khatami, M. A review on metal-organic frameworks: Synthesis and applications. *TrAC Trends Anal. Chem* **2019**, *118*, 401−425.
(22) Anik, Ü.; Timur, S.; Dursun, Z. Metal organic frameworks in electrochemical and optical sensing platforms: a review. *Microchim. Acta* **2019**, *186*, 1−15.
(23) Wang, K. B.; Xun, Q.; Zhang, Q. Recent progress in metal-organic frameworks as active materials for supercapacitors. *EnergyChem.* **2020**, *2*, No. 100025.
(24) Gautam, S.; Agrawal, H.; Thakur, M.; Akbari, A.; Sharda, H.; Kaur, R.; Amini, M. Metal oxides and metal organic frameworks for the photocatalytic degradation: A review. *J. Environ. Chem. Eng.* **2020**, *8*, No. 103726.
(25) Khan, N. A.; Hasan, Z.; Jhung, S. H. Adsorptive removal of hazardous materials using metal-organic frameworks (MOFs): a review. *J. Hazard. Mater.* **2013**, *244-245*, 444−456.
(26) Remya, V. R.; Kurian, M. Synthesis and catalytic applications of metal−organic frameworks: a review on recent literature. *Int. Nano Lett.* **2019**, *9*, 17−29.
(27) Du, M.; Li, Q.; Zhao, Y.; Liu, C. S.; Pang, H. A review of electrochemical energy storage behaviors based on pristine metal−organic frameworks and their composites. *Coord. Chem. Rev.* **2020**, *416*, No. 213341.
(28) Jiang, J. Computational screening of metal− organic frameworks for CO_2 separation. *Curr. Opin. Green Sustainable Chem.* **2019**, *16*, 57−64.
(29) Pandey, A.; Dhas, N.; Deshmukh, P.; Caro, C.; Patil, P.; García-Martín, M. L.; Padya, B.; Nikam, A.; Mehta, T.; Mutalik, S. Heterogeneous surface architectured metal-organic frameworks for cancer therapy, imaging, and biosensing: A state-of-the-art review. *Coord. Chem. Rev.* **2020**, *409*, No. 213212.
(30) Shen, M.; Forghani, F.; Kong, X.; Liu, D.; Ye, X.; Chen, S.; Ding, T. Antibacterial applications of metal−organic frameworks and their composites. *Compr. Rev. Food Sci. Food Saf.* **2020**, *19*, 1397−1419.
(31) Lee, Y. R.; Kim, J.; Ahn, W. S. Synthesis of metal-organic frameworks: A mini review. *Korean J. Chem. Eng.* **2013**, *30*, 1667−1680.
(32) Bian, Y.; Xiong, N.; Zhu, G. Technology for the remediation of water pollution: A review on the fabrication of metal organic frameworks. *Processes* **2018**, *6*, 122.
(33) Liang, S.; Wu, X. L.; Xiong, J.; Zong, M. H.; Lou, W. Y. Metal-organic frameworks as novel matrices for efficient enzyme immobilization: an update review. *Coord. Chem. Rev.* **2020**, *406*, No. 213149.
(34) Liu, K.; Zheng, Y.; Jia, G.; Yang, M.; Song, Y.; Guo, N.; You, H. Nano/micro-scaled La (1, 3, 5-BTC)$(H_2O)_6$ coordination polymer: Facile morphology-controlled fabrication and color-tunable photoluminescence properties by co-doping Eu^{3+}, Tb^{3+}. *J. Solid State Chem.* **2010**, *183*, 2309−2316.
(35) Kumar, S.; Jain, S.; Nehra, M.; Dilbaghi, N.; Marrazza, G.; Kim, K. H. Green synthesis of metal−organic frameworks: A state-of-the-art review of potential environmental and medical applications. *Coord. Chem. Rev.* **2020**, *420*, No. 213407.
(36) Kumar, S.; Jain, S.; Nehra, M.; Dilbaghi, N.; Marrazza, G.; Kim, K. H. Green synthesis of metal−organic frameworks: A state-of-the-art review of potential environmental and medical applications. *Coord. Chem. Rev.* **2020**, *420*, No. 213407.
(37) Mu, B.; Walton, K. S. Thermal analysis and heat capacity study of metal−organic frameworks. *J. Phys. Chem. C* **2011**, *115*, 22748−22754.
(38) Liu, J. W.; Zhang, Y.; Chen, X. W.; Wang, J. H. Graphene oxide−rare earth metal−organic framework composites for the selective isolation of hemoglobin. *ACS Appl. Mater. Interfaces* **2014**, *6*, 10196−10204.
(39) Prabhu, S. M.; Imamura, S.; Sasaki, K. Mono-, di-, and tricarboxylic acid facilitated lanthanum-based organic frameworks: insights into the structural stability and mechanistic approach for superior adsorption of arsenate from water. *ACS Sustainable Chem. Eng.* **2019**, *7*, 6917−6928.
(40) Laurikenas, A.; Beganskiene, A.; Kareiva, A. On the Synthesis and Characterization of Lanthanide Metal-Organic Frameworks. *Ceramics* **2018**, *1*, 54−64.
(41) Li, Y.; Zhong, Y.; Huang, J. The synthesis of a lanthanum metal−organic framework and its sensitivity electrochemical detection of H_2O_2. *Chem. Pap.* **2017**, *71*, 913−920.
(42) Zhang, X.; Sun, F.; He, J.; Xu, H.; Cui, F.; Wang, W. Robust phosphate capture over inorganic adsorbents derived from lanthanum metal organic frameworks. *Chem. Eng. J.* **2017**, *326*, 1086−1094.
(43) Jeyaseelan, A.; Kumar, I. A.; Viswanathan, N.; Naushad, M. Development and characterization of hydroxyapatite layered lanthanum organic frameworks by template method for defluoridation of water. *J. Colloid Interface Sci.* **2022**, 228.

https://doi.org/10.1021/acsomega.2c03973
ACS Omega 2023, 8, 262−270

(44) Paz, F. A. A.; Klinowski, J.; Vilela, S. M.; Tome, J. P.; Cavaleiro, J. A.; Rocha, J. Ligand design for functional metal−organic frameworks. *Chem. Soc. Rev.* **2012**, *41*, 1088−1110.
(45) Lin-Vien, D., Colthup, N. B., Fateley, W. G.; Grasselli, J. G. *The handbook of infrared and Raman characteristic frequencies of organic molecules*; Elsevier. 1991.
(46) Cano, A.; Monroy, I.; Ávila, M.; Velasco-Arias, D.; Rodríguez-Hernández, J.; Reguera, E. Relevant electronic interactions related to the coordination chemistry of tetracyanometallates. An XPS study. *New J. Chem.* **2019**, *43*, 18384−18393.
(47) Furlani, C.; Polzonetti, G.; Preti, C.; Tosi, G. XPS of coordination compounds: data on the electronic structure of a series of Cu (II) N, N′-cyclic substituted dithiocarbamates. *Inorg. Chim. Acta* **1983**, *73*, 105−111.
(48) Elanchezhiyan, S. S.; Prabhu, S. M.; Kim, Y.; Park, C. M. Lanthanum-substituted bimetallic magnetic materials assembled carboxylate-rich graphene oxide nanohybrids as highly efficient adsorbent for perfluorooctanoic acid adsorption from aqueous solutions. *Appl. Surf. Sci.* **2020**, *509*, No. 144716.
(49) Muthu Prabhu, S.; Chuaicham, C.; Sasaki, K. A mechanistic approach for the synthesis of carboxylate-rich carbonaceous biomass-doped lanthanum-oxalate nanocomplex for arsenate adsorption. *ACS Sustainable Chem. Eng.* **2018**, *6*, 6052−6063.
(50) Mane, V. J.; Malavekar, D. B.; Ubale, S. B.; Bulakhe, R. N.; In, I.; Lokhande, C. D. Binder free lanthanum doped manganese oxide@ graphene oxide composite as high energy density electrode material for flexible symmetric solid state supercapacitor. *Electrochim. Acta* **2020**, *335*, No. 135613.
(51) Atuchin, V. V.; Gavrilova, T. A.; Grivel, J. C.; Kesler, V. G. Electronic structure of layered ferroelectric high-k titanate $La_2Ti_2O_7$. *J. Phys. D: Appl. Phys.* **2009**, *42*, No. 035305.
(52) Anusha, T.; Bhavani, K. S.; Kumar, J. S.; Brahman, P. K. Synthesis and characterization of novel lanthanum nanoparticles-graphene quantum dots coupled with zeolitic imidazolate framework and its electrochemical sensing application towards vitamin D_3 deficiency. *Colloids Surf., A* **2021**, *611*, No. 125854.
(53) Du, M.; Zhao, X. J.; Wang, Y. Crystal engineering of a versatile building block toward the design of novel inorganic−organic coordination architectures. *Dalton Trans.* **2004**, 2065−2072.
(54) Qian, D.; Xu, B.; Cho, H. M.; Hatsukade, T.; Carroll, K. J.; Meng, Y. S. Lithium lanthanum titanium oxides: a fast ionic conductive coating for lithium-ion battery cathodes. *Chem. Mater.* **2012**, *24*, 2744−2751.
(55) Balusamy, B.; Kandhasamy, Y. G.; Senthamizhan, A.; Chandrasekaran, G.; Subramanian, M. S.; Kumaravel, T. S. Characterization and bacterial toxicity of lanthanum oxide bulk and nanoparticles. *J. Rare Earths* **2012**, *30*, 1298−1302.
(56) Zheng, Q.; Zhang, Y.; Montazerian, M.; Gulbiten, O.; Mauro, J. C.; Zanotto, E. D.; Yue, Y. Understanding glass through differential scanning calorimetry. *Chem. Rev.* **2019**, *119*, 7848−7939.
(57) Bimbo, N.; Zhang, K.; Aggarwal, H.; Mays, T. J.; Jiang, J.; Barbour, L. J.; Ting, V. P. Hydrogen Adsorption in Metal−Organic Framework MIL-101 (Cr)—Adsorbate Densities and Enthalpies from Sorption, Neutron Scattering, In Situ X-ray Diffraction, Calorimetry, and Molecular Simulations. *ACS Appl. Energy Mater.* **2021**, *4*, 7839−7847.
(58) Boguta, P.; Sokołowska, Z.; Skic, K. Use of thermal analysis coupled with differential scanning calorimetry, quadrupole mass spectrometry and infrared spectroscopy (TG-DSC-QMS-FTIR) to monitor chemical properties and thermal stability of fulvic and humic acids. *PLoS One* **2017**, *12*, e0189653.
(59) Boutin, A.; Bousquet, D.; Ortiz, A. U.; Coudert, F. X.; Fuchs, A. H.; Ballandras, A.; Weber, G.; Bezverkhyy, I.; Bellat, J. P.; Ortiz, G.; Chaplais, G.; Paillaud, J. L.; Marichal, C.; Nouali, H.; Patarin, J. Temperature-induced structural transitions in the gallium-based MIL-53 metal−organic framework. *J. Phys. Chem. C* **2013**, *117*, 8180−8188.
(60) Banerjee, D.; Wang, H.; Gong, Q.; Plonka, A. M.; Jagiello, J.; Wu, H.; Woerner, W. R.; Emge, T. J.; Olson, D. H.; Parise, J. B.; Li, J. Direct structural evidence of commensurate-to-incommensurate transition of hydrocarbon adsorption in a microporous metal organic framework. *Chem. Sci.* **2016**, *7*, 759−765.
(61) Longley, L.; Collins, S. M.; Li, S.; Smales, G. J.; Erucar, I.; Qiao, A.; Hou, J.; Doherty, C. M.; Thornton, A. W.; Hill, A. J.; Yu, X. Flux melting of metal−organic frameworks. *Chem. Sci.* **2019**, *10*, 3592−3601.
(62) Mu, B.; Walton, K. S. Thermal analysis and heat capacity study of metal−organic frameworks. *J. Phys. Chem. C* **2011**, *115*, 22748−22754.
(63) Sotomayor, F. J.; Cychosz, K. A.; Thommes, M. Characterization of micro/mesoporous materials by physisorption: concepts and case studies. *Acc. Mater. Surf. Res* **2018**, *3*, 34−50.
(64) Wang, F.; Deng, K.; Wu, G.; Liao, H.; Liao, H.; Zhang, L.; Lan, S.; Zhang, J.; Song, X.; Wen, L. Facile and large-scale syntheses of nanocrystal rare earth metal−organic frameworks at room temperature and their photoluminescence properties. *J. Inorg. Organomet. Polym. Mater.* **2012**, *22*, 680−685.

https://doi.org/10.1021/acsomega.2c03973
ACS Omega 2023, 8, 262−270